ENGINEERING MR TECHNOLOGY FOR LOW-COST PORTABLE DEVICE DESIGN

An Undergraduate Research Scholars Thesis

by

JOHN BERLIEN

Submitted to the Undergraduate Research Scholars program
Texas A&M University
in partial fulfillment of the requirements for the designation as an

UNDERGRADUATE RESEARCH SCHOLAR

Approved by
Research Advisor: Dr. Steven Wright

May 2016

Major: Electrical Engineering

TABLE OF CONTENTS

ABSTRACT

Engineering MR Technology for Low-Cost Portable Device Design

John Berlien
Department of Electrical and Computer Engineering
Texas A&M University

Research Advisor: Dr. Steven Wright
Department of Electrical and Computer Engineering

Magnetic Resonance Imaging is an invaluable tool used in many fields, and is a mainstay of medical imaging. Conventional MRI scanners are impractical to move and prohibitively expensive, weighing thousands of pounds and costing upwards of a million dollars. Thus, conventional approaches to MRI may be limiting the applications of this important technology. It is possible, using rare-earth magnets (FeNdB), to create a lightweight, portable, and low cost magnet suitable for Nuclear Magnetic Resonance (NMR) and MRI. We have developed two prototype magnets, using the concept of a Halbach array and the NMR-MANDHALAS method described by Peter Bluemler et al. Constructed of 3D-printed parts and identical cubic magnets, the prototypes have a 0.27 T field with a 5 mm spherical region of approximately 300 parts-per-million (ppm) homogeneity and a 0.18 T field with a 5 mm region of 2000 ppm before shimming. Relatively easy to assemble and safe for handling, these prototype magnets have the potential to enable portable MRI and other Magnetic Resonance experiments.

DEDICATION

I dedicate this work to my fiancé, Lauren, who is my inspiration and my everything.

ACKNOWLEDGMENTS

I'd like to thank firstly Dr. Wright, who has helped me learn so much during my research. I'd also like to thank the graduate students in the Magnetic Resonance Systems Lab at Texas A&M, who have remained patient with me through my endless questions. Finally, I'd like to thank Jim Wilson and those at the Engineering Innovation Center at Texas A&M for all of their help.

CHAPTER I

INTRODUCTION

Magnetic Resonance, or more aptly nuclear magnetic resonance (NMR), is a phenomenon on which much of today's imaging technology is based. The most common and familiar application of this technology is the Magnetic Resonance Imaging (MRI) machine. These room-sized machines are indispensable for modern medicine, enabling doctors to obtain clear images of inside the human body for improved diagnoses and other information. However, these machines require very large and powerful magnets in order to produce the needed magnetic fields. The larger the field, the clearer the image. These magnets, and the machines to house and utilize them, are always very expensive, limiting the number of MRI machines and the like being made and used to hospitals and universities, mostly. However, it is possible to use smaller magnets to produce smaller, albeit less powerful, imaging machines. They can draw very little power in comparison to large MRI machines, and the smaller size lends to a high portability. These smaller machines could be used in a wide variety of applications, namely identifying the chemical makeup of an object being scanned. It is for this application that a small, very portable, even wearable, device can be created to measure the chemical makeup of the blood or some other object in the body. However, there are many challenges involved in creating such a machine.

Basics of Magnetic Resonance Imaging

Magnetic Resonance Imaging is a very complex process, involving many components. Briefly explained in this section is how MRI works and the basic components involved.

Nuclear Magnetic Resonance (NMR)

Nuclear Magnetic Resonance, as previously stated, is the phenomenon on which MRI is based. Understanding this concept completely involves very complex mathematics and quantum physics, but a rudimentary understanding is sufficient for the purposes of this thesis.

On the subatomic level, protons have a property called spin. There are a couple models that illustrate this, and the classical model is the most intuitive, and therefore used here. According to the classical model, the protons are actually spinning (this is only a model, particles do not spin). The spinning atoms create a small magnetization. Most particles in an atomic nucleus have two spin states: spin up or spin down. This important distinction is revisited later. In the presence of a static, homogeneous magnetic field, called B_0 (pronounced B naught or B zero), the direction of these spins will align with the direction of the magnetic field. The rate at which the spins are precessing is dependent only on the type of nucleus and the strength of the magnetic field. The ratio of the angular velocity of the spins to the strength of the magnetic field is known as the gyromagnetic ratio, and is specific to each atom. For example, the gyromagnetic ratio of hydrogen-1 (1H) is 2.675×10^8 radians/s/T, or 42.576 MHz/T. Frequency is more often used in MRI than angular velocity, so the gyromagnetic ratio is often seen in units of Hz/T. The frequency of the precession of the spins in a certain magnetic field is called the Larmor frequency. For example, for 1H in a 3T field, a field strength common in modern clinical MRIs, the Larmor frequency is 127.728 MHz. Most frequencies used in various MRI systems are in what is called the Radio Frequency (RF) range.

Now is when we must define the coordinate axes to systematically describe the direction of the spin magnetization. If we describe the magnetization as simply a vector, we can say that in the presence of a static magnetic field, the vector is mostly aligned with the direction of the magnetic field. Conventionally, in an xyz coordinate system, the z direction is the direction of the static magnetic field. With the magnetization mostly in the z direction, "spinning" around the z axis at the Larmor frequency, another external magnetic field, called B_1, can be applied, perpendicular to the z axis, that would "tip" the spins farther away from the z axis, due to vector addition. This brings the spins into an excited state, and as they return to equilibrium (back toward the z axis), the magnetization creates a time-varying magnetic field. To illustrate, we will say that the amount that the spins are tipped (called the tip angle) is enough to bring the spins completely onto the xy plane, which would be a 90-degree tip angle, since the x-y plane is 90 degrees from the z axis. This also means that the magnetization in the z direction is zero. If B_1 were just a short, static magnetic field, the magnetization would simply be strongest in the direction of B_1. However, if B_1 is varied sinusoidally in some direction in the x-y plane, *at the same frequency of the spins*, then the magnetization is successfully tipped by B_1. This is because when the magnitude of B_1 is a sinusoid, becoming positive and negative at the same rate as the magnetization is spinning, then the magnitude of B_1 is following the direction of the magnetization vector. This means that when an external magnetic field B_1 is created that varies at the Larmor frequency of a particle, then the spins of those particles are excited and create time-varying magnetic fields as they return to equilibrium, which creates a voltage difference (and current in a conductor) due to Faraday's Law of Induction; this is the essence of NMR. When we have a static magnetic field, and create an external magnetic field varying at the Larmor frequency, we can detect the magnetization of the spins of the particles (such as Hydrogen-1).

FIDs and spin echoes

The very basic part of MRI is interacting with the magnetization of particles, which was explained in the previous section. With a static magnetic field, we create a perpendicular magnetic field that varies at the Larmor frequency, referred to as an RF pulse. Even though RF pulse is typically thought of as an electromagnetic pulse in the Radio Frequency, this is not an electromagnetic pulse. This is simply referred to as an RF pulse because Larmor frequencies are typically in the RF range. When an RF pulse tips the spins, and the spins create detectable time-varying magnetic fields, we measure these and call them Free Induction Delays (FIDs). Since this FID varies with the Larmor frequency, we take the data as an envelope, which is the curve describing the max value of the FID. This envelope is shaped as an exponential decay function. The FID decays for two reasons. One reason is an effect called proton-proton shielding, which is due to some spins being in a spin up state and some being in a spin down state. This decay is unavoidable, but helpful, as it is characteristic of certain materials. This decay is called T_2 decay, as the equation for the envelope of the FID ideally can be described as an exponential decay with a T_2 time constant. However, there is another source of decay: the inhomogeneity of the magnet. This is one of the biggest issues in MRI, and one of the biggest limitations. In order to have an image that is of reasonable quality, the homogeneity of the static magnetic field must be on the order of 100 parts per million (ppm), or 0.01%. *This means that the strength of the magnetic field cannot vary more than 0.01% in the area being imaged*. More details on this limitation will be discussed later. The decay of the FID due to the inhomogeneity of the magnet is referred to as T_2* decay (pronounced tee two star), which actually describes the exponential decay of the envelope. T_2* decay is larger than T_2, which presents a problem. Since T_2 is a characteristic of

substances such as certain tissues, or changes when cancer is present, it is important that we are able to detect T_2. Therefore, we devise a way to overcome T_2* decay in order to measure T_2. Some time after we generate an RF pulse with, say, a 90-degree tip angle, we generate a second pulse with a 180-degree tip angle. This pulse "flips" the spins, and the time-varying magnetic field decaying at T_2 is essentially revived. This is called a spin echo, as it "echoes" the FID. By measuring the maximum value of the spin echo, we can use this to find T_2, assuming an exponential decay envelope across the FID and echo.

The frequency domain and gradient coils

Finding T_2 is useful, but the image reconstruction process is done in what is called the frequency domain. Once spin echoes are obtained, they can be seen in what is called the time domain. This is the normal signal, what one would detect and observe. Using the Fourier Transform, it is possible to see the frequency data in the spin echo. Frequency data refers to the magnitudes of the signal at different frequencies. To help understand this, for illustrative purposes we can say the magnetic field is perfectly homogeneous. There would be only one field strength possible, and thus only one Larmor frequency. In the frequency domain, we would only see data at one point, the Larmor frequency. However, since no field is perfectly homogeneous, we see a large amount of the magnitude of the signal at the middle Larmor frequency, and some signal around the Larmor frequency, since variation in the field strength also causes variation in the Larmor frequency, due to their direction relationship. Therefore, in the echo, a peak is observed at the Larmor frequency, and how much it varies around the Larmor frequency is determined by the homogeneity of the magnetic field.

This concept of inhomogeneity causing the Larmor frequency to change was expanded on by Paul Lauterbur to use NMR to create images [1-3]. Lauterbur intentionally caused inhomogeneity in the field in order to spatially represent objects. This is done through gradient coils. Gradient coils cause a linear inhomogeneity in the magnetic field, called a gradient, larger than the already-present inhomogeneity, in order to frequency encode the spatial position of objects. Frequency encoding just means that each position in space corresponds to a certain Larmor frequency, and since the variation of the field (and thus frequency) is linear, frequency is easily translated into spatial data. When an echo is taken while gradients are applied, the result in the frequency domain is called a projection. A projection is a one-dimensional representation of a two-dimensional image. When displayed graphically, the x axis of the projection represents the frequency (translating into position) and the y axis represents the magnitude of the signal, or the amount of "stuff" along the orthogonal axis at a particular position.

Image reconstruction

Once projections are obtained, there are multiple methods of image reconstruction in MRI. The first method, called projection reconstruction, was simply rotating the object and obtaining projections at each angle. This method is also used by CT (computed tomography) scanners, which simply have an apparatus that takes an X-ray projection at a given angle and then rotates to a different angle to obtain the next projection. Once projections are obtained at the desired number of angles, a mathematical tool called an inverse Radon transform is used to reconstruct the image using projections at different angles.

The second method of image reconstruction is the far more common in modern MRI scanners (as it would be difficult to rotate a person/object inside the scanner): using multiple gradient coils. This involves having three types of gradient coils, one for each direction (x, y, and z). The gradient coil previously discussed that helps to obtain the projection by encoding space to frequency is called the frequency encoding (FE) gradient. The other two gradients are the slice select gradient and the phase encoding (PE) gradient. The slice select gradient simply determines where the "slice" (section of the object being imaged) is and the slice thickness. The phase encoding gradient is what moves the frequency encoding gradient along the axis perpendicular to the projection in order to obtain projections two-dimensionally. It does this by changing magnitude for every projection obtained. Choosing which gradient coil corresponds to which gradient type is rather arbitrary – it only depends on what type of slice is desired.

The projections are then mapped out onto what is called k space, which is a two-dimensional plot representing the frequency domain data of an image. Along one axis is the frequency encoding gradient, and along the other axis is the phase encoding gradient, with the magnitude of the projections being represented by brightness. The interaction between the frequency encoding gradient and the phase encoding gradient can be easier imagined on this k space plot: along the frequency encoding axis is the position of the projection, and the magnitude is represented by brightness. The phase encoding gradient essentially shifts the frequency encoding gradient along the phase encoding axis, allowing for another projection to be obtained at that point on the phase encoding axis along the frequency encoding axis. Once a k space plot is obtained, ideally a two-dimensional inverse Fourier Transform is used to convert the data into an image.

Hardware components of MRI

Once a basic understanding of the process behind MRI is achieved, the next step is to understand the components of an MRI scanner.

Magnet

The most important component in an MRI scanner is the magnet. The magnet generates the main static magnetic field that aligns the spins of the particles of interest. There are multiple types of magnets used in MRI, with superconducting wire magnets being by far the most common in clinical scanners. These magnets use large coils of superconducting wire, which is essentially wire with very low loss of energy due to resistance. This wire is super-cooled with liquid cryogen agents such as liquid nitrogen and liquid hydrogen. When a current is applied to the coils, they generate a magnetic field along the axis through the center of the coil. This means that to generate a magnetic field, these magnets have to be powered constantly. These materials that make up the superconducting magnet are very expensive, and the continued cost of the cooling agents also increases the expense over time.

Another alternative type of magnet is one that is probably more familiar: a permanent magnet. A permanent magnet is made of metal or stone, and constantly creates its own magnetic field. A simple example of this is a refrigerator magnet. These are not quite so commonly used in MRI, as they generally cannot produce a field strong or homogeneous enough needed for clinical and other uses. However, there are a subset of applications in which permanent magnets perform very well.

Radio-Frequency (RF) coil

The next part of the MRI scanner is the RF coil. The main function of this coil is directly interacting with the different spins inside of the object being scanned. It generates the external magnetic field, oscillating at the Larmor frequency, that is perpendicular to the main magnetic field in order to tip the spins. It then detects the magnetic field generated by the digressing spins. There are several different configurations for RF coils. One common in clinical MRI scanners is the birdcage coil. The RF coil is placed inside of the magnet assembly, around the object being scanned, in order to generate a magnetic field around the entire object.

Gradient coils and shim coils

Also inside the magnet assembly with the RF coil are the gradient coils. Gradient coils, as discussed in the previous section, generate gradients which produce a linear variation in the magnetic field, allowing for localization of a signal. There is a coil for each axis of the coordinate system: x, y, and z.

Gradient coils are also used in a process called shimming. Shimming creates a more homogeneous field by adding additional magnetic fields in the x, y, and z directions. The magnetic fields created by the coils are opposite from the field variations, cancelling out inhomogeneity. Gradient coils create linear field variations, so they are called first-order shims. Additional shim coils are added to create higher order shims. In order to produce the most homogenous field possible, an MRI scanner could have many shim coils.

Amplifiers, switches, gates, and mixers

The rest of the MRI scanner involves relatively simple, basic components in a setup similar to a radar system. The easiest way to explain the rest of the components is to go through the process of an MRI acquisition pulse sequence.

First, a pulse sequence generator (PSG) keeps the timing of the RF and gradient pulses in line. This is often not a computer, but a dedicated processor, since a computer is performing many tasks simultaneously and any interrupt to the program can disrupt the timing, corrupting the scan. Using the PSG, the RF pulses and gradient pulses are being driven. To protect the components and to ensure that only the correct signals are being passed through, a process called gating limits when a component is enabled. The RF pulses go through a mixing stage, where the frequency of the pulse is raised to the Larmor frequency, and amplified before being sent to the RF coil. Simultaneously, the gradient pulses are amplified (significantly more so than the RF pulses) and are sent to the gradient coils. Once a signal is received by the RF coil, it is met by what is called a Transmit/Receive (T/R) switch, which protects the components of the system. It is then amplified and mixed down to a lower frequency to limit strain analog to digital converter (ADC), and digitized so that the data can be sent to and stored on a computer.

It is possible for much of this to happen in software, if power requirements are low and high-quality equipment is used. For example, if a the Larmor frequency of the magnet is low enough, it is not necessary to add a mixing stage, the PSG can directly drive the RF pulses at this frequency.

Challenges of MRI

Magnetic Resonance Imaging is a versatile and fantastic imaging modality, but even it has drawbacks. Most often used MRI scanners are clinical scanners and research-centered university scanners. Like Computed X-Ray Tomography (CT), these a large, nearly immobile machines, and quite heavy. They also require quite a large amount of power. Not only does the superconducting magnet need to be constantly powered, but the main source of power consumption is the gradient coils, which consume kilowatts (kW) of power during a scan. The high fields inside and even near the superconducting magnet can also be quite dangerous. Anything magnetic can suddenly fly into the magnet if brought too close. And finally, perhaps the biggest issue with MRI, is the expense. The magnet of a clinical MRI scanner alone costs approximately $1 million per Tesla (T), with clinical scanners using normally 1.5 T or 3 T. This limits the number of available MRI scanners, as usually only hospitals and universities can afford these machines. Unfortunately, since these machines are necessary for medical research and diagnoses, this raises the health care cost for the average person, and especially so if their physician requires a high-resolution MRI image to confirm a diagnosis. Decreasing the cost of these machines could decrease the cost of health care overall. When anything but the highest quality of image in the body is required, a portable, low-cost solution to heavy, expensive, and power hungry MRI scanners could be found.

Goals of this project

The ultimate goal of this project, simply, is to create a complete portable MRI system. This would include three main stages: building or finding a magnet, implementing RF hardware and necessary coils for data acquisition, and portability optimization.

The first stage is the most important and possibly the most difficult, as the magnet is the most important part of an MRI system. It is also the biggest limiting factor – the other components of the system can be made to be as large or as small as needed relatively easily. This includes both the physical magnet and shimming. This thesis discusses this first stage, including the physical magnet(s) and some shimming.

The plans for the next stage of the project involve using what is called Software-Defined Radio (SDR). SDR is a type of software and hardware that involves RF signal processing at low cost. It is typically open-source, which means that the software is free to use and the hardware schematic is common-knowledge, allowing customization and addition to the software and hardware.

The final stage of the project involves optimization of the design, e.g. implementing battery power or temperature insulation of the magnet. This would be what could be called “finishing touches.”

CHAPTER II

METHODS

The methods of this project have been very fluid and transient, changing at almost every turn. A certain flexibility was necessary, due to the novelty of the project, both in the literature and in the Magnetic Resonance Systems Lab at Texas A&M. Although the idea behind this project has recently become a more popular topic among magnetic resonance engineers, methods previously used in other experiments had to be tailored to our specifications.

Previous methods for portable MRI

Before explaining the methods used for this project, it is important to first review methods previously used to create portable NMR and MRI scanners. The methods explained here are both influential in later methods and in this project.

NMR-MOUSE

One of the first and most successful attempts at a portable NMR device was the NMR Mobile Universal Surface Explorer (NMR-MOUSE) [4-6]. The NMR-MOUSE is a one-sided NMR device that produces a relatively large and homogeneous field to conduct NMR experiments on possibly large objects. It works using two semi-cylindrical magnets with antiparallel axial magnetization, with a solenoidal RF coil perpendicular to the main magnetic field. This creates an inhomogeneous gradient field across a surface being measured, and allows for spatial encoding with no gradient coils. This is so innovative because it lends itself to high portability and the NMR scanning of the surface of arbitrarily large objects and surfaces.

Desktop MRI

A popular approach to low-cost, portable MRI is using a desktop magnet [7-9]. Desktop magnets are permanent magnets that are very light compared to a superconducting magnet, but still quite heavy for a normal person to carry around. These are often C-magnets, which are two plate magnets held some distance apart by a heavy yoke, usually iron. These are relatively weak and not very homogeneous, especially a significant distance away from the center. However, they make good educational tools, and were an important advancement in portable MRI.

NMR-Mandhalas

A couple of papers by Peter Bluemler et al., one of those that worked on the NMR-MOUSE, revolutionized portable MRI with a method of producing magnets with strong, homogeneous fields: the Mandhalas (Magnet Arrangements for Novel Discrete Halbach Layout) method [10]. This method uses Halbach arrays (explained below) stacked together to create a magnet that produces a magnetic field that is homogeneous [11]. This method is now used very often in portable NMR [12].

NMR-CUFF

There are numerous uses for portable NMR and MRI, as demonstrated by the NMR-MOUSE. One of these uses is for plants – specifically, branches and stems of plants. One example of this is the MRI machine built for outdoor measurements of trees [13]. Another example is the NMR-CUFF (Cut open, Uniform, Force Free), a complete MRI scanner that is actually hinged and can be opened and closed around an object [14]. This is ideal for scanning thin plant stems.

Portable MRI scanner without gradient coils

One of the more recent big innovations in portable MRI was done by Clarissa Zimmerman-Cooley et al. [15, 16]. What is unique about this project is that it does not need gradient coils – it uses spatial encoding with a specifically inhomogeneous field in the spatial encoding direction. Instead of phase encoding, the magnets mechanically rotate around the sample to acquire projections (as discussed in the introduction). This is unconventional, as most MRI scanners today implement phase encoding, as opposed to rotation, and use Fourier reconstruction. However, without gradient coils, the power requirement is dramatically decreased, lending to a higher portability than a similarly-sized scanner with gradient coils.

Magnet

The magnet, as seen through previous examples of portable MRI, is probably the biggest limitation in MRI. Magnets in clinical scanners are superconductive, large and power-hungry. It would be nearly impossible to create a smaller, portable, low-cost version of this. This severely limits the potential of MRI, since the superconducting magnet system is the main type of system that is widely used to gather data. Although there are desktop scanners available, the magnets are still heavy and bulky, not to mention relatively weak and inhomogeneous. Constructing a portable, handheld magnet that is sufficiently strong and that can be made sufficiently homogeneous in itself is no trivial matter.

Constraints

There were several sets of constraints agreed on before constructing a magnet. When considering MRI in general, the two most important constraints are the field strength and homogeneity. If a

stable structure is created and these constraints are met, then other constraints, such as cost, are secondary. However, in this case, there are several other constraints that are equally important. In order to be considered a complete success, the project must meet constraints: field strength, homogeneity, inner aperture size, weight, and cost. The field strength agreed upon had to be at least 0.3 Tesla, although this constraint was changed later in favor of a higher homogeneity. The field homogeneity, ultimately, had to be close to 150 ppm for imaging, but this would only be achieved after shimming. Homogeneity was defined as field variation over a volume size designated for imaging, which was decided to be somewhere between 0.5 cm diameter sphere and 1 cm diameter sphere. Inner aperture size was decided to be at least a diameter of 2 cm, as other equipment such as shim coils, gradient coils, and an RF coil had to also fit inside, in addition to whatever was being imaged. The weight constraint was set to be less than 12 lbs was acceptable, and less than 10 lbs was ideal. Portable is a broad term that could have several definitions, such as “can be moved” or “lab on a chip” [17, 18]. For this project, portable is defined as “handheld.” A fully-enclosed MRI magnet has to be at least as large as the volume of the object being imaged. The cost constraint was not clearly defined, since the cost of the magnet would not be nearly as high as that of a superconducting magnet. However, cost was compared between possible methods, and was still a factor in making decisions about which methods were chosen.

Ideas considered

When considering how to obtain a magnet suitable for the project, there were two different choices to make. One choice was to use either a permanent magnet or electromagnet. An electromagnet would limit the portability of the device, complicate the process, and possibly

increase the cost. A permanent magnet setup was therefore chosen. The second choice was to either find and purchase an electromagnet, or to create one. This choice required further deliberation.

The first magnet that was considered was the PM 1055-050N, found on the GMW Associates website. It is a small, palm-sized magnet with a tiny aperture of 32x14 mm. This, however, would've been too small for our purposes. This would've been difficult to measure anything larger than a vial of blood or perhaps even a finger. It would've been almost impossible to fit gradient coils inside the aperture, and thus this could not be used for MR imaging. It was also significantly expensive, costing over $4000. These magnets are unfortunately also made-to-order, without any kept in stock. This would have taken 6-8 weeks to deliver the magnet from the time of ordering, a significant amount of time considering the entire temporal scope of the project is approximately 8 months.

Further investigation into finding a different, more suitable magnet was done, but no magnet was found. Instead, focus shifted to building the magnet. This would allow much more compatibility with our standards.

Once the decision to build the magnet was made, methods of magnet construction were investigated. First, a traditional C-shaped two-plate magnet was considered. This kind of magnet is traditionally used in desktop systems, and even in some experimental systems, such as open full-body MRI scanners, designed for those with limiting conditions, e.g. claustrophobia or obesity [19]. However, this kind of magnet is bulky, heavy, and relatively weak and

inhomogeneous. Further research in the literature was done and a different method was found: using a Halbach array.

Halbach cylinder

A Halbach array is a configuration of permanent magnets that creates a strong, homogeneous field in one area and near zero field outside of that volume [20]. Specifically, for an MRI magnet, a dipolar Halbach cylinder would be used. The principle behind a dipolar Halbach cylinder is that for a given angle of rotation around the cylinder, the angle of rotation of the magnetization vector of the magnet is doubled; this is shown in Fig. 1 [10].

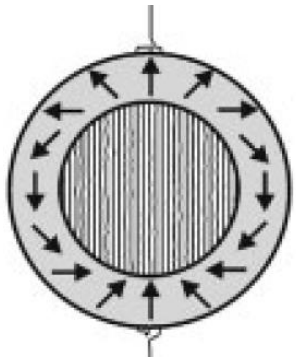

Fig. 1: Halbach configuration. Adapted from Fig. 1b of [10].

This cannot be actually realized, but an approximation is possible when the cylinder is discretized, as shown in Fig. 2.

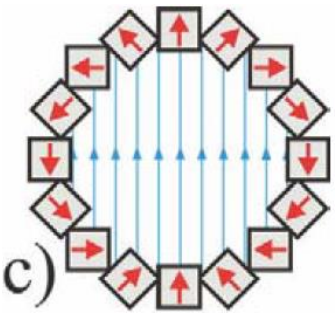

Fig. 2: Discretization of Halbach cylinder. Adapted from Fig. 1c from [11].

This discretization is realized with identically-shaped permanent magnets arranged in a circle, with the distance between the center of the cylinder and the center of each magnet staying constant. The arrangement of the magnetization vectors of the magnets must also follow the principle behind the Halbach cylinder; that is, their angles of rotation must be double their rotation around the center of the cylinder.

The advantages of using a Halbach cylinder are many, especially when the cylinder can be discretized into identical permanent magnets. The main advantage is the field that is produced – it is relatively strong and homogenous for a permanent magnet setup. It is also simple to assemble and to design. There is also no need for a yoke, as in C-shaped permanent magnets. This decreases the weight and bulkiness. Depending on the type of magnets purchased, it is also relatively inexpensive for a magnet setup of its size (the size depending on whatever the user chooses). This appeared to be ideal for our purposes, and is often used in portable NMR and MRI experiments [21-23].

Magnet design

Once the decision was made to construct a Halbach cylinder magnet formation, using the NMR-Mandhalas method devised by Bluemler et al., an optimization was needed to fit our constraints [10]. Unfortunately, as it often is with MRI, an improvement with one parameter has a negative effect on another parameter, i.e. there is always a tradeoff. For example, increasing the homogeneity of the field by increasing the discretization of the cylinder decreases the strength of the field, for a given fixed radius; or for a fixed strength and homogeneity, increasing the radius increases the size of the magnets and thus the cost.

The main decision involved the number associated with discretization. This number is defined by how many magnets are in the circle creating the face of the cylinder. A project by Windt et al., the NMR-CUFF, has a discretization of four, denoted in the Mandhalas method as n=4 [14]. This discretization, while creating a strong and unexpectedly homogeneous field, requires relatively large magnets when compared to the aperture size, and becomes rather restrictive, allowing for only small samples. For the NMR-CUFF project, when the samples were often only thin plant stems, this suited their purposes quite well. For the MRSL, this would add difficulty in creating a complete imaging machine when needing to fit three sets of gradient coils (for three dimensions) and an RF coil inside the aperture. While this would certainly be possible, as shown in the NMR-CUFF experiment, it would be easier to begin our experiment with a larger aperture size.

To compare the fields created by different discretization, or ‘n’, values, a 2D magnetostatic software was used called FEMM 4.2. N values of 8, 16, 24, and 32 were considered. The shape of the individual magnets was chosen to be a square for simplicity (Fig. 3).

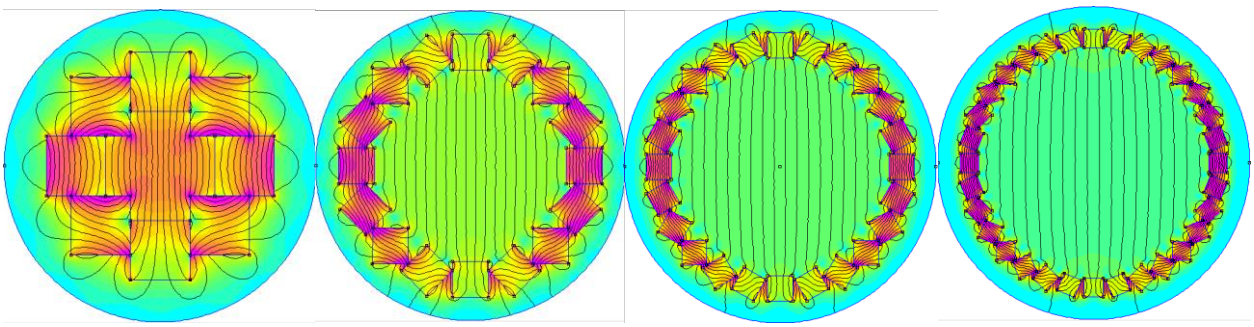

Fig. 3: Magnetic field simulations for different n values

An n-value of 8 was soon discarded due to its high level of inhomogeneity, and n=32 provided too little advantage of homogeneity, if any, over 24 to justify its low field strength. A table (Table x) was created with values comparing each design, and the decision was made to eventually create both n = 16 and n = 24, but starting with n = 16.

Table 1: Potential magnet comparison table

Property	n = 8	n = 16	n=24	n=32
Magnet size	3/4 "	7 mm	1/4"	3/16"
Center field strength	0.8 T	0.32 T	0.213 T	0.152 T
Max Aperture size	2.7 cm	3.42 cm	5.33 cm	5.68 cm
Weight	7.39 lbs	0.73 lbs	0.82 lbs	0.462 lbs
Cost	$489.28	$62.77	$152.60	$112.64
Structure size	8.08 cm	5.39 cm	7.13 cm	7 cm
Homogeneity (over 1cm)		5096 ppm	2968 ppm	3129 ppm
Homogeneity (over r_innner/10)		610.7 ppm	131.5 ppm	1000 ppm

The values differ slightly from the hypothetical n = 16 magnet to the actual magnet, as the individual magnets used were 3/8 inches to a side.

Magnet formers

One of the more challenging and time-consuming aspects of the project was the construction of the magnet formers – the structure(s) that would hold the individual magnets in place. The NMR-Mandhalas method simplified this by outlining a process of creating essentially "stacks": n magnets would be arranged in a circle according to the Halbach cylinder, and this would count as one layer [11]. Multiple layers would be created to be stacked on top of one another to increase the field strength and homogeneity in the direction along the cylinder.

Initial Design

Using the NMR-Mandhalas method, a design was created in software before coming to life in hardware. At first, laser-cutting the formers was considered. Plastic was thought to be possibly strong enough to withstand the forces of the magnets, so a simple design was created to test this. Equations for the geometry of the design were adapted from the Mandhalas method, and a MATLAB program was written to calculate the exact parameters. The design was drawn in AutoCAD, a Computer-Aided Design software meant mostly for 2D applications. Since laser-cutting plastic involves cutting 2D plates of plastic, this program was well-suited. It was also required for the woodshop/laser cutting facility on Texas A&M campus.

For the 3D printed parts, a new file or reused file from AutoCAD was created in another CAD software called SolidWorks. SolidWorks is much more suited towards 3D part design, and was therefore the preferred software when designing 3D-printed parts. With the help of those at the EIC, the 3D parts were created and printed.

Creation of stacks

In the NMR-Mandhalas paper by Bluemler et al., aluminum casing was used for the magnets, the case divided in half to create a “sandwich”, as shown in Fig. 4.

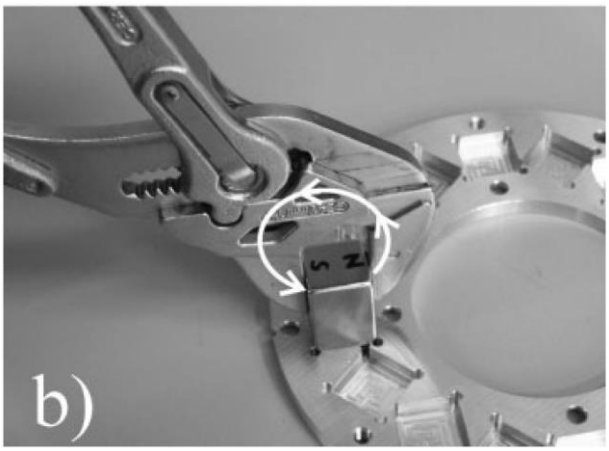

Fig. 4: Mandhalas magnet stack half. Adapted from [10].

An epoxy was used to keep each magnet in its individual slot during the process of inserting the magnets. This is necessary due to the forces the individual magnets exert on each other.

Although aluminum would have been the highest quality nonmagnetic readily available material to use, it would also have been one of the more expensive options, not to mention more difficult to machine. One of the first alternatives to consider was laser-cutting plastics instead of machining aluminum. Assuming such a material could be sufficiently strong, this was thought to be a good alternative. Not only would plastic be a cheaper option and easier to construct, but it would eliminate a common NMR issue called eddy currents. Eddy currents are a result of changes in magnetic field creating a current in a conductive material, such as most metals, including aluminum. These currents would then induce a magnetic field, creating unwanted

perturbations in the main magnetic field. Any metal used in the final assembly would conduct electricity and therefore possibly create eddy currents, so conductive materials were avoided if at all possible.

After deciding to try laser-cutting plastic, the material needed to be chosen. There are advantages and disadvantages with each material, so choosing the right one ideal for our project was important. It was imperative that this material be strong, but it would also be ideal that it wouldn't be easily breakable. Unfortunately, a strong, rigid material such as acrylic or Lexar would be more easily breakable than a more flexible material.

The initial design implementing laser-cutting would require the slot parts for the magnets to be cut, and then two caps on each end of the slot pieces would hold the magnets in place. The slot parts for the magnets were to be 3/8-inch-thick, the same size as the magnets for the n=16 configuration. The cap pieces on either side were to be 1/32-inch thick. The original design was circular, offering no obvious way to attach the stacks together. After having this design made as a test run, it became immediately obvious that laser-cutting would not work for the purposes of this project. The issue was that there are areas between each magnet where the distance between the magnets decreases essentially to zero thickness of the material, which is difficult to achieve in reality. The laser-cutting process just simply did not cut fine enough to achieve an acceptable result in this regard.

When it became obvious that laser-cutting would not be adequate, it was decided that 3D printing would be the next option. First, it was necessary start prototyping one stack before

creating all eight. Jim Wilson at the Engineering Innovation Center (EIC) at Texas A&M took care of creating the prototypes at the 3D printing lab in the EIC. The first prototypes were made of Fullcure amber acrylic and white ABS plastic. The acrylic resulted in an accurate print, but the ABS print was not quite accurate enough. The tricky part for the printing lay in the tapering thickness where the magnets touch – this results in a zero thickness, which is difficult for even a higher quality 3D printer.

The 3D printed parts had two types: magnet slots, and cap pieces. The magnet slots were square, with about 82 mm to each side, and had a thickness of 10.5 mm. The thickness of the magnet slots was chosen to be 1/32 inch thicker than the magnets themselves, which were 3/8 inch. The magnet slots also have 3/8 inch square slots for the magnets, arranged in a circle around the center with orientations appropriate for a Halbach array. There was also a center hole, 39 mm in diameter, for the bore. In each corner, there was a ¼ inch hole for a threaded brass rod. The cap pieces were similar, but had only the quarter inch holes and the center hole, no slots. Additionally, they were 1/32-inch-thick, creating a space of 1/32 inch on each side of the magnets along the axis of the bore (x axis).

Originally, the magnets were to be glued or epoxied into the slots, and the cap pieces glued on top. This is a design that is permanent in nature, and in anticipation of future issues, this was not the final design. Instead of glue, it was decided that the magnets would simply sit in the slots, and the cap pieces would be held on by a screw and nut. In four places, there was one hole for a screw to fit through the cap and into the magnet slot. On the other side, in the bottom of the magnet slot, a hex nut would sit inside a hexagonal hole, and the screw would be affixed to this

nut. This keeps the cap pieces in place during construction, and also allows a “retrievable” design. There were also small 1 mm holes in each slot in the magnet slot pieces, to allow something small (in this case the end of a mechanical pencil) to push out the magnet from the bottom up and out to be retrieved. This also increases ease of construction and eliminates the need for glue or epoxy. This retrievable design becomes important when future issues inevitably occur.

The stacks are connected by four brass rods passing through all eight completed stacks. The stacks are then held in place by sets of two brass nuts on both ends of each brass rod (eight total). Sets of two nuts were used to ensure that the stacks would be held in place. The first iteration can be seen in Fig. 5.

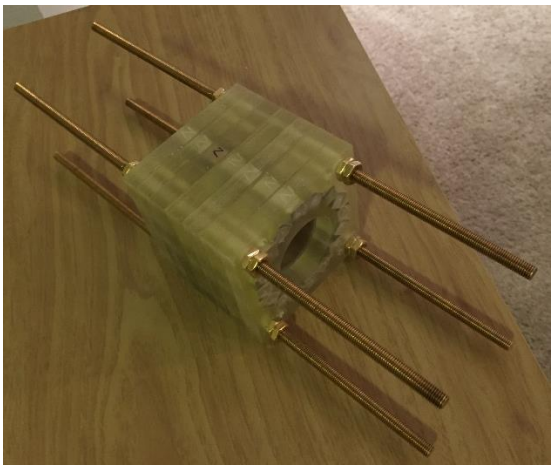

Fig 5: First iteration of n = 16 magnet.

Final assembly

One of the biggest problems encountered thus far was when the entire magnet was assembled. It was evident that not only were there forces between the individual magnets in each stack, but

there were forces acting between each stack as well. Since the stacks essentially acted as dipoles (magnets with two poles), each stack would repel the stack next to it. This would have been difficult to predict without advanced 3D magnetostatic simulation software. This would not have been a problem if the acrylic pieces had been more rigid, but since the pieces were not solid all the way through the middle, as this would defeat the purpose of the magnet, there was a weak point where there was less material. This allowed the forces acting between the stacks to push out the magnets from the center. At first this was a minor bulge, but the pieces continued to give way until every piece was irreparably warped. This required a replacement of every piece, as they had all been compromised.

Different measures had to be taken for the second iteration of the magnet assembly. Any warping of the magnet formers could result distortion of the field. This, however, could be fixed during the shimming process. The main issue was continuous movement of the pieces due to the magnetic forces. This would not only change the field itself, but make it much more difficult to correct with shimming; therefore, a solution had to be found.

There were several steps to counteracting the warping problem. The first and perhaps most intuitive step was to simply add pieces on both ends of the assembly. Since the magnet slot pieces were thinner in the slot areas, the structure of the pieces was weaker than that of a piece that would be solid all way through. Thus a solid piece should add sufficient stability to the assembly and thus prevent warping. These end pieces were created in SolidWorks and printed along with the other parts of the assembly.

The second step was to try a different material. The first material used was Fullcure 720, a translucent amber acrylic. This material is adequate for prototyping, as it is a cheaper material used by the EIC, but for the final assembly, there are other materials that are better-suited. The material used had to not only be quite strong, to withstand the forces of the magnets, but also extremely rigid. The pieces could not be allowed to flex – flexing pieces would not only lead to warping, but continuous movement. A more rigid material (and more expensive) used by the EIC was called VeroWhite, a white, more opaque material than Fullcure 720. VeroWhite also has a higher strength and rigidity than Fullcure 720. The second set of magnet formers for assembly was then printed in this new material.

A unique property of several types of 3D printing acrylic material is that the curing process involves ultraviolet (UV) light. This means that UV light is used to harden the material during the print. Fortunately, even after printing, UV light can be utilized to further cure the material. The final step taken to counteract warping was to leave the completed parts in sunlight for several days. This was later revealed to be a critical step in ensuring rigidity in the parts.

After all these steps were taken, the magnet was reassembled using the new parts and old magnet material. Because of the retrievable design, the magnets were relatively easy to extract from the old assembly and insert into the new assembly. Once the new assembly was built, the pieces did not move at all. Thus the warping problem appeared to have been fixed. The second iteration can be seen in Fig. 6.

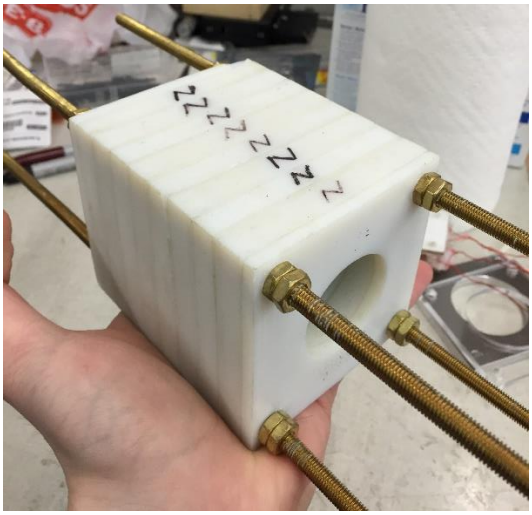

Fig. 6: Second iteration of the n = 16 magnet.

Second magnet

After the magnet was constructed, its homogeneity was measured to be around 360 ppm in a 5 mm cubic region (a discussion of the measurement process is below). Upon measuring this, it was clear that shimming would need to be done. A higher homogeneity, at least as good as 100 ppm, would be required for imaging. Then the idea was presented to merely create a second magnet with a higher homogeneity. Since the material had already been acquired for a second magnet with a discretization of 24, the decision to create a second magnet with a (hopefully) higher homogeneity was easy. This new magnet with higher homogeneity would be a better starting point when beginning the shimming process.

There were also other benefits to the second magnet in addition to a higher homogeneity. The biggest benefit was a larger aperture size. Since the magnets used were smaller (1/4 inch to a side) for the second magnet, they were not only less strong but also allowed more space in the

middle of the magnet, because of the much smaller volume. The smaller volume also led to a significant decrease in weight.

Starting with the leftover AutoCAD file already created for these magnet formers, a conversion to SolidWorks and the adding of details was necessary for the next 3D printing. Simple enough with the help of those at the EIC, new parts were quickly constructed in SolidWorks and printed. The completed second magnet is shown in Fig. 7.

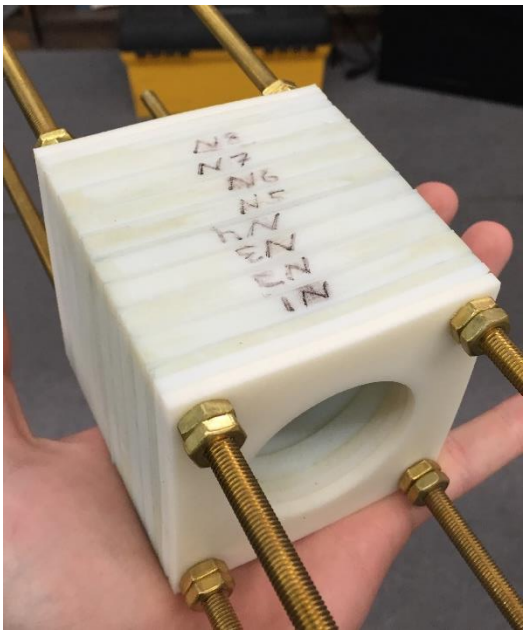

Fig. 7: Completed second magnet.

However, with a deadline approaching at this particular point in the project, it was important to have results of the second magnet, which did not allow time for additional curing of the parts in UV light. This led to the parts being fairly flexible, even the end pieces. Quickly more end pieces were printed in various materials, including VeroWhite, ABS plastic, and a sturdy, yet

apparently flexible material called Endur. Even when these three materials were stacked on top of each other, it still allowed some bending of the slot pieces, mostly on the ends of the magnet. This issue can be seen in Fig. 8.

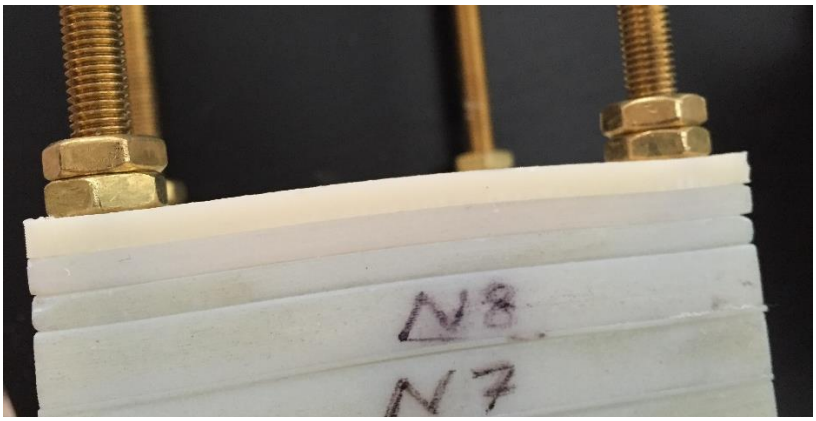

Fig. 8: Flexible end-pieces problem.

Homogeneity measurement

The homogeneity of each magnet was measured using a 3D positioner and a Gaussmeter, as shown in Fig. 9.

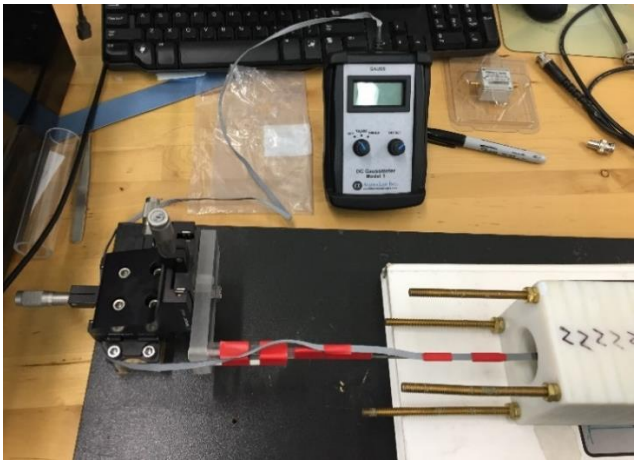

Fig. 9: Homogeneity measurement setup.

The 3D positioner had 3-axis fine-tune position adjustment, at a cost of limited range. A Gaussmeter is simply a probe to measure the strength of a magnetic field in Gauss (G). A Gauss is 10^{-4} Tesla, and to put into perspective, the Earth's magnetic field is approximately 0.5 Gauss in magnitude. Attaching the Gaussmeter probe to the end of the 3D positioner and inserting this into each magnet, magnetic field magnitude values were taken at hundreds of points to obtain an idea of the shape of the field in the future possible imaging region. The values were recorded in Excel and analyzed in MATLAB to create a surface plot (3D representation) of the field variation. Once the shape of the field variations was obtained, the next important step would be to use this knowledge as a guide during shimming.

Obtaining a spin-echo

The spin-echo pulse sequence, as described in the introduction, is the go-to NMR experiment when testing a magnet for its NMR-related capabilities. An attempt was made to evaluate the magnet in this way.

Micro-coil NMR experiment

The method originally suggested to be used for measuring homogeneity in the first magnet was the implementation of a micro-coil. A micro-coil is a type of RF coil used for finding field values over a small volume. To create this, thin wire was wrapped around a glass capillary tube that was filled with water and sealed with wax on either end. This coil had approximately 70 turns (wrapped around the tube 70 times).

The next step was creating what is called a matching network. Since most devices operate at an electrical impedance of 50 Ohms (Ω), it is important that connecting devices and antennas (the RF coil behaves as an antenna) that their impedances are also matched, in order to minimize power loss. If the electrical impedance between two devices is not matched, i.e. not the same, then a significant amount of electrical power will be lost and not all power transmitted from one device will reach the next. A matching network using a circuit of capacitors is created to match the RF coil impedance to 50 Ω. This is done efficiently by measuring the impedance of the coil by itself, using what is called a network analyzer, and then using a program to find capacitor values to use in the matching network circuit. In this case, the software used was called Smith V3.10, developed by Fritz Dellsperger of Bern University.

Once a matching network circuit was created, a process called tuning fine-adjusts the capacitor values, if the capacitors are variable capacitors, to as closely match 50 Ω as possible and limit power loss. This is done by adjusting each capacitor, and alternating the adjustment of each until a 50 Ω impedance is achieved.

The other frequency-dependent device is the T/R switch. A passive T/R switch, meaning it requires no external power, is frequency-dependent because of its use of capacitors and inductors. Therefore, a T/R switch needs to be adjusted to each frequency, or a new T/R switch must be built for a new frequency. A T/R switch was created using diodes and inductors.

The rest of the echo-acquisition setup was not frequency-dependent, and therefore could be used at any frequency. This was convenient, as the Texas A&M course ECEN 463: Magnetic

Resonance Engineering, implements such a setup for desktop permanent magnets. This setup involves National Instruments (NI) hardware, for Digital-to-Analog Conversion (DAC) and digitizing, and NI software for programming the spin-echo pulse sequence, as shown in Fig. 10.

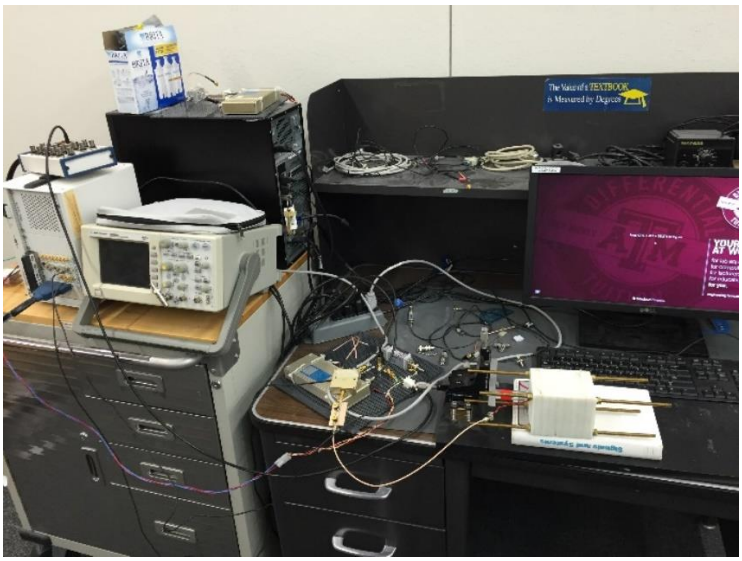

Fig. 10: Spin-echo acquisition setup.

Since this course had already been completed, files were already available for obtaining a spin-echo sequence.

Shimming

A preliminary attempt at shimming was also done on the second magnet. A shim coil set was actually constructed, using a paper by Anderson [24]. This paper describes a method of correcting field inhomogeneity using electrical current shims by creating two identical sets of planar (flat) gradient coils. Designs for both first order (linear) and second order (quadratic) coils are included. Using dimensions provided in the paper, which are based on separation different

between the planar sets, an image was created in MATLAB of the entire coil set, as shown in Fig. 11, and printed out to scale.

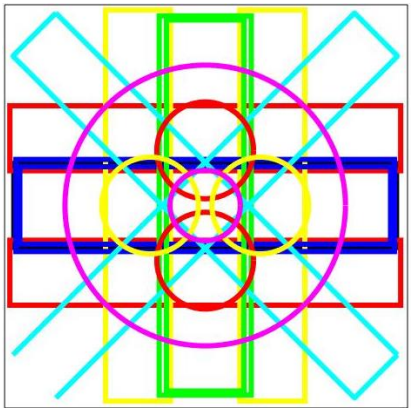

Fig. 11: Shim coil MATLAB image.

Each color represents one type of coil configuration, e.g. yellow represents a coil that generates a field in the Y direction, and magenta represents a coil that generates a field in the "direction" $2Z^2 - X^2 - Y^2$. Multiple configurations in one color represent different options for that direction, e.g. for the Y direction, either the rectangular or circular coils could be used (but not both).

The paper image was then attached to cardboard, with push pins inserted at corner points. Magnet wire was then wound around these push pins 5 turns (with one exception of 6 turns), and taped in place onto the paper image. Each coil requires an input and output wire, and these must lead from an outside setup to the inside of the magnet, through the coil, and return out again. Sometimes unfortunately, any current in a wire causes a magnetic field, which could perturb either the main magnetic field or the shimming fields. The wires are therefore twisted together to help minimize this. The setup thus far is seen in Fig. 12.

Fig. 12: One side of shim coil setup.

Coil sets were placed in series. Once the coil sets were wound and taped, the paper image was transferred from the cardboard to a stronger, more rigid backing. Holes were then drilled into the corners of the shim sets and nylon screws inserted through the holes. Four nylon hex nuts on each screw were used as spacers to keep a 1 cm distance. Screws were secured with nylon hex nuts on the opposite side of the apparatus. The completed shim set is shown in Fig. 13. In this setup, just as a preliminary step, only second-order shims are included, as the field variations are largely quadratic, as seen in the results section.

Fig. 13: Completed shim coil setup.

A circuit is needed to regulate the current in the shim coils. A preliminary design was drawn, as seen in Fig. 14.

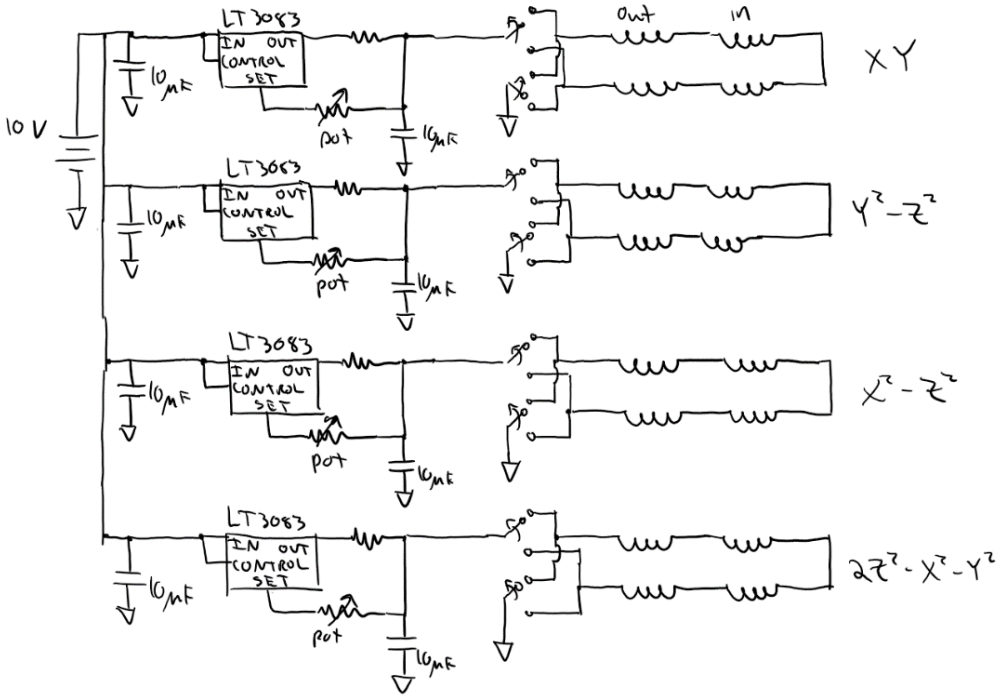

Fig. 14: Hand-drawn schematic of shimming circuit configuration.

This circuit uses the adjustable voltage regulator LT3083 from Linear Technologies in a current source configuration. This regulates the current using a voltage drop across a potentiometer. It also uses switches to change the direction of the current through the coil, allowing either a positive or negative field.

Shimming will be done using the completed setup, and adjusting the current in each shim coil by adjusting each potentiometer until a minimum homogeneity is found (around 150 ppm). The homogeneity will need to be measured by a spin-echo NMR experiment, from which the homogeneity can be calculated. The homogeneity will be calculated from the echo by measuring the linewidth of the frequency response of the echo using a full-width half maximum (FWHM) method. The NMR experiment will run continuously, allowing feedback from an adjustment approximately every second.

Passive shimming

Also done were preliminary plans to implement passive shimming methods. Passive shimming involves the systematic placement of magnetic materials to correct magnetic fields. This is almost always done to permanent magnets as a primary means of correcting the field. Unfortunately, placing small magnetic pieces of material, often steel or iron, in order to correct the field is very complicated. Often advanced software is required to predict where these pieces will go. In this case, instead of steel or iron, more small magnets would be placed to create a field variation opposite to that of the main magnetic field. Simulation was done again in FEMM 4.2, and the results are shown in Fig. 15.

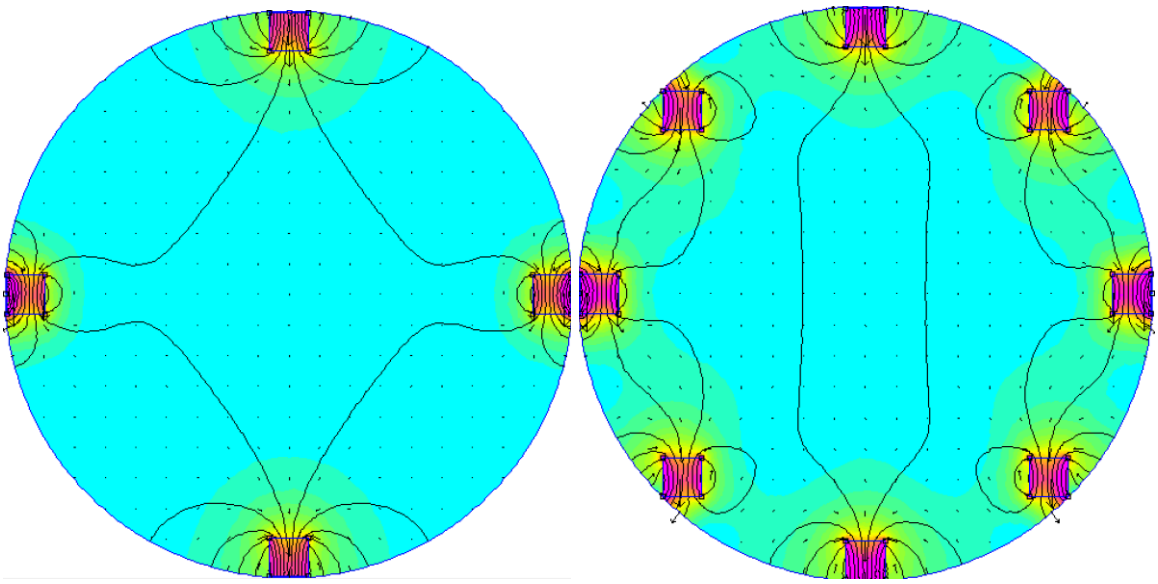

Fig. 15: Passive shimming method preliminary design.

There would be two rings of these magnets, each placed some equal distance from the center.

There are several possible issues with this design. The biggest issue is that the magnitude of the field created by these magnets is fixed, and can be changed only by the size of the magnets, or possibly their distance from the center of the complete magnet.

CHAPTER III

RESULTS

The results of the project can be stated relatively briefly. The type of project in this case leaned more toward design than experiment.

Magnets

The results from the first magnet were measured mostly in strength and homogeneity, but other parameters are notable as well. The main goals of course were imaging-quality characteristics of the magnet.

What is also important to note when considering results is to compare them across similar projects, to determine the validity of this project.

Magnet field strength and homogeneity

The strength of the magnetic field of the first magnet is approximately 2778 Gauss (G), or 0.2778 Tesla (T). This characterizes the strength of the "center field", which defines the very center of the magnet. It is determined to be where the gradient field (the change in magnetic field) is approximately zero. This is broken down into a maximum field strength in the x-direction, a maximum field strength in the y-direction, and a minimum field strength in the z-direction.

The homogeneity of the field before shimming is approximately 360 ppm in a 5 mm spherical region. By this, meaning that the Gaussmeter reading did not vary more than 1 Gauss in this region. A more accurate measurement is difficult to achieve with the probe that was used. This could indicate a different homogeneity value, somewhere possibly between 300 – 500 ppm. Values were taken at various points using the 3D positioner and Gaussmeter, and entered into Microsoft Excel. An analysis was done in MATLAB, and a surface plot of the field in the y-z plane was created, as shown in Fig. 16.

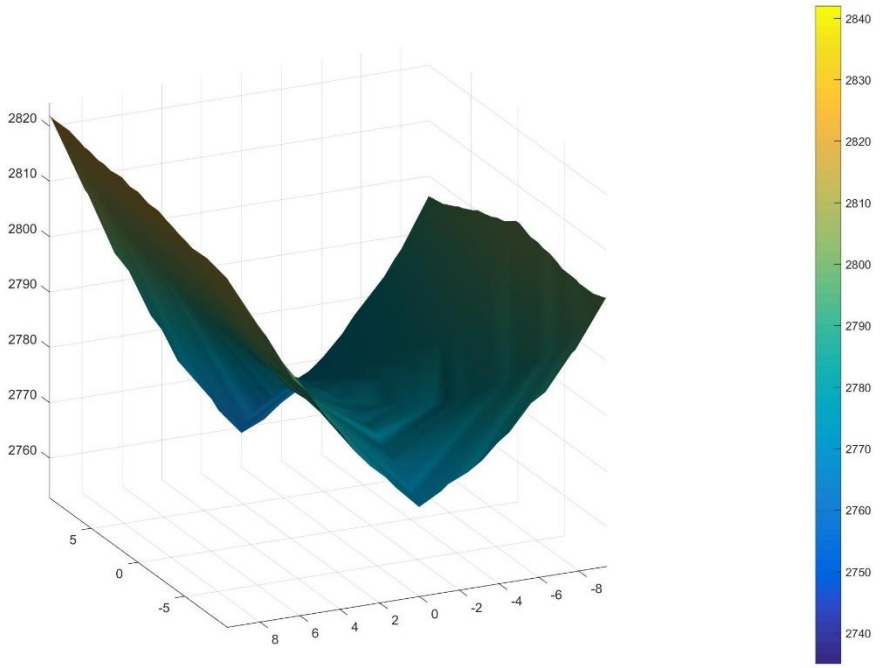

Fig. 16: Field plot (y-z plane) for first magnet.

The same was done for the second magnet, as shown in Fig. 17. The center field was found to be 1539.5 Gauss. The field varies about 10-12 Gauss in a 5 mm cubic region, which indicates a homogeneity of about 2000-4000 ppm.

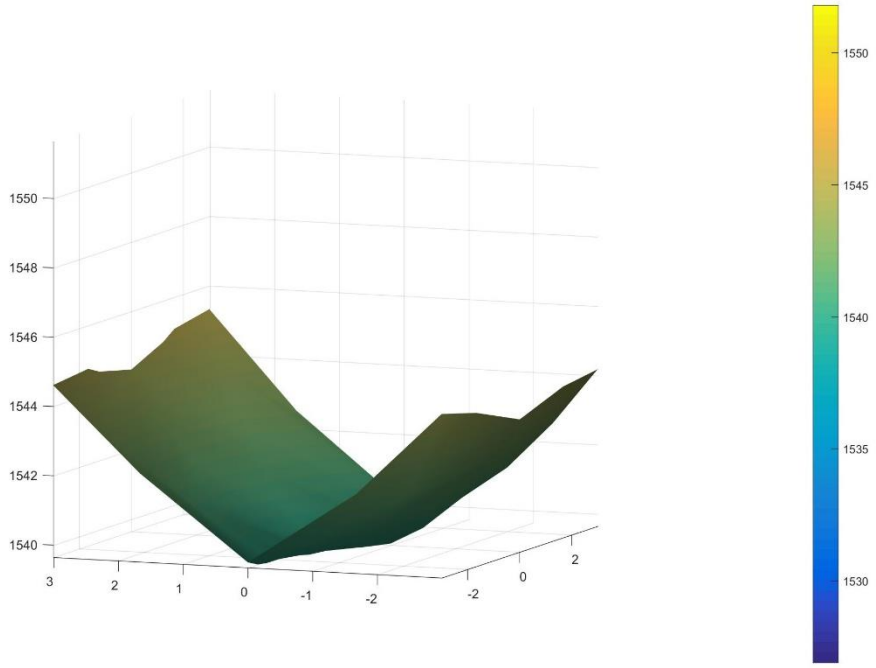

Fig. 17: Field plot (y-z plane) for the second magnet.

The units for the spatial directions are in mm, and the field strength is in Gauss.

CHAPTER IV

CONCLUSION

This project has demonstrated some interesting results, and this and other projects in portable MRI have encouraging implications.

Homogeneity

Although the field strength was about as expected, considering that the field simulations were for infinitely long magnets, the homogeneity measurements yielded surprising results: namely that the second magnet appeared to be *less* homogeneous than the first magnet. This is surprising, since one would expect a higher homogeneity from a higher discretization number. There are a couple possible reasons for this. One is found by looking at the different field shapes of the two magnets. For the first magnet, the center field seems to be a minimum in the z-direction but a maximum in the y-direction. The quadratic shapes of the fields in these directions could possibly be cancelling each other out in the center, creating a relatively large region of homogeneity. For the second magnet, the center field seems to be a minimum in both the y and z directions, and thus the quadratic shaped fields add to each other instead of cancelling out, decreasing the homogeneity in the center. This could have something to do with the choice of discretization number,

Another possible explanation, although less likely, is the length of each magnet. Although both magnets have 8 stacks, the first magnet has larger individual magnets, so each stack is thicker in the first magnet. This means that the first magnet is significantly longer than the second, which

leads to an increased homogeneity in the x-direction (along the length of the magnet). It could possibly lead to an increased homogeneity in the y- and z-directions, though after a cursory examination of each stack of the second magnet with the positioner/Gaussmeter testing, this does not appear to be the case.

Another possibility is simply in the design or construction. The second magnet could have been constructed incorrectly, though again after the testing of each stack, this is not likely. The magnets could possibly be simply too small, and the

This is a troubling find, but the second magnet could still be used as a development platform for shimming and gradient coils. However, it appears that the first magnet is more advantageous when acquiring FIDs, echoes, and ultimately images.

Comparison with similar projects

The previous portable MRI project most similar to this is the NMR-CUFF. The NMR-CUFF is a complete, hand-held MRI scanner using a Halbach array, much like the goal of this project. Comparing results, the NMR-CUFF was able to achieve a homogeneity of 50 ppm over a 5 mm spherical volume using passive shimming methods, including 1 mm steel polecaps and iron platelets.

Comparing the results of this project with the NMR-CUFF, it could be said that the results are somewhat encouraging, mostly for the n = 16 magnet. Of course, the measurements taken are

before shimming, so there is confidence that the results achieved by the NMR-CUFF could also be achieved for this project as well.

There are several significant differences between this project and other projects, such as the NMR-CUFF. One is that low cost and a relatively simple and robust design are high priorities in this project. This is why methods such as 3D printing are used instead of more expensive options such as machining aluminum. A low-cost design is very important, not only in development, but in possible applications. This design is also simple enough to be relatively easily replicated. It was already replicated once, with a second iteration of the first magnet. An idea behind this project is to make not only the magnet easily replicated but also the rest of the scanner.

Another difference is that the goal of this project is an entire system, not just a scanner. This includes the magnet, hardware, and console to control it. The plan is to design and create a complete portable MRI system.

Current status and future plans

Currently, this project is still in phase 1. Sufficient shimming, which would be marked by an achievement of 150 ppm over a potential imaging region (between 5 mm and 10 mm spherical volume), would mark the end of phase 1. Ideally sometime in phase 2, shimming would be implemented in software using an optimization routine, with a console driving control voltages and amplifiers converting the voltages to currents. Phase 2 would consist of acquiring SDR hardware to replace the NI components used in the NMR acquisition setup (Fig. x) and programming pulse sequences into SDR software. Ideally, at the end of phase 2 there would be a

complete hand-held MRI scanner that implements SDR hardware and software. Phase 3 would consist of an optimization of the design, considering other portability factors such as temperature insulation, portable RF shielding, battery power, and fast image acquisition.

Possible applications

There are many possible applications for low-cost portable MRI. One of the most important possibilities that should be discussed is scalability of this (or any) project. An interesting characteristic of a Halbach array is that, for a given n-value, the field strength remains the same for any size (theoretically). This means that the design could ideally be scaled to be any desired size. This is shown in Zimmerman-Cooley's magnet and one of Bluemler's magnets; the Halbach array can be made to be any size [10, 15]. Of course, there are complications to consider, such as the danger of dealing with large, powerful permanent magnets. This would require significant care; as permanent magnets can be quite dangerous. Another complication is the power required by larger gradient coils. This is obviously considered in Zimmerman-Cooley's work, but for other works that use gradient coils, a larger head- or even body-sized magnet would require large amounts of power for the gradient coils, similar to that of a conventional scanner. Although this might save some on cost, it would be more difficult to make portable. However, the possibility still remains of a design for a scanner built to scan a finger could be scaled to one built to scan a hand, or a head.

If a portable low-cost scanner such as these could be built, it could have widespread implications. If a physician could have a simple MRI machine in his/her office for obtaining low to medium quality images, it could dramatically decrease global health care costs.

It could also be used as an educational tool. If every university could have an MRI instruction class, where students could construct and program their own scanners, more students could learn about MRI and the field itself could expand.

Ultimately, low-cost portable MRI is possible, if not inevitable, and has endless possibilities. The goal of this project is to help realize this.

APPENDIX

This appendix serves to better show the design of the magnet formers.

For the n = 16 magnet, images of the cap piece and slots piece are shown in Fig. A1.

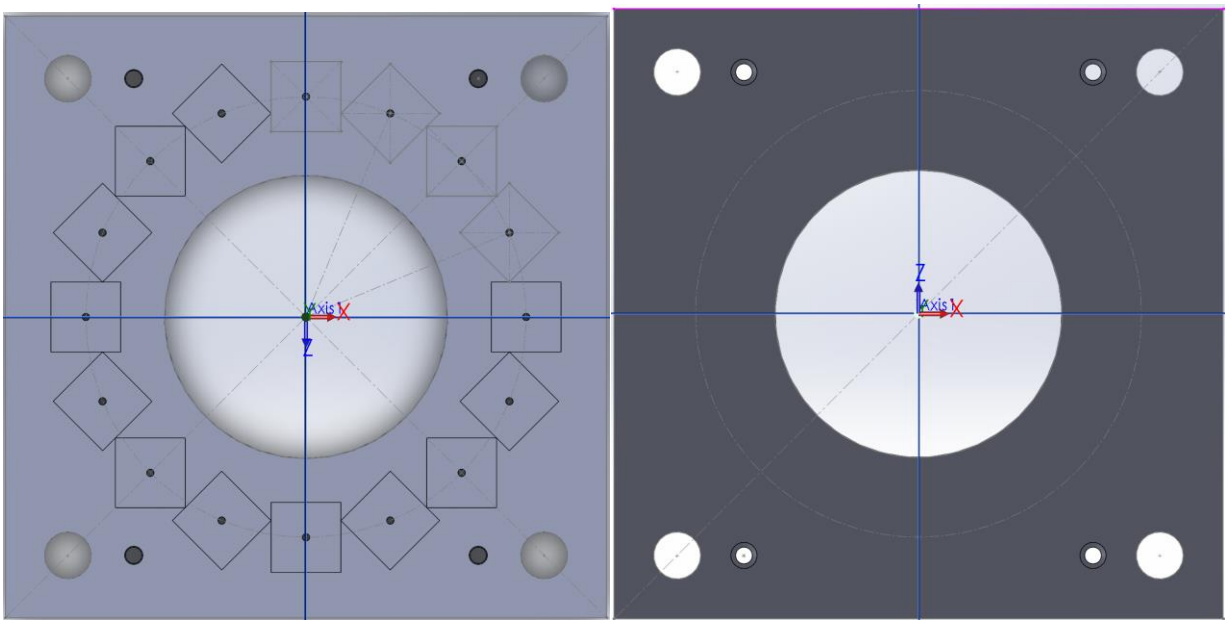

Fig. A1: n = 16 magnet former drawings.

For the slots, the squares are actually 3/8 inch cubic holes. The holes in the corners are ¼ inch to allow for ¼ inch brass rods. The circular hole in the center is 38.63 mm in diameter. The length and width are 82.02 mm. The screw holes are created using the SolidWorks hole wizard, using the #2 flat head machine screw (100) type hole. The hole begins in the cap piece, and is raised in the slot piece to accommodate for the cap piece. The cap piece is 1/32 inches thick and the slot

piece is 7/32 inches thick. There are holes on the other side of the slot pieces, as shown in Fig. A2, for the hex nuts. These are also created using the hole wizard.

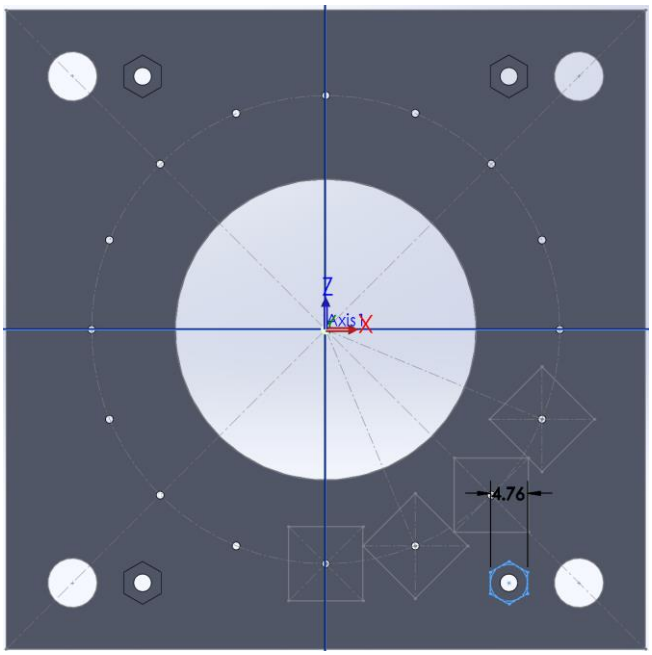

Fig. A2: Slot piece reverse side.

Similar drawings for the n = 24 magnet are shown in Fig. A3.

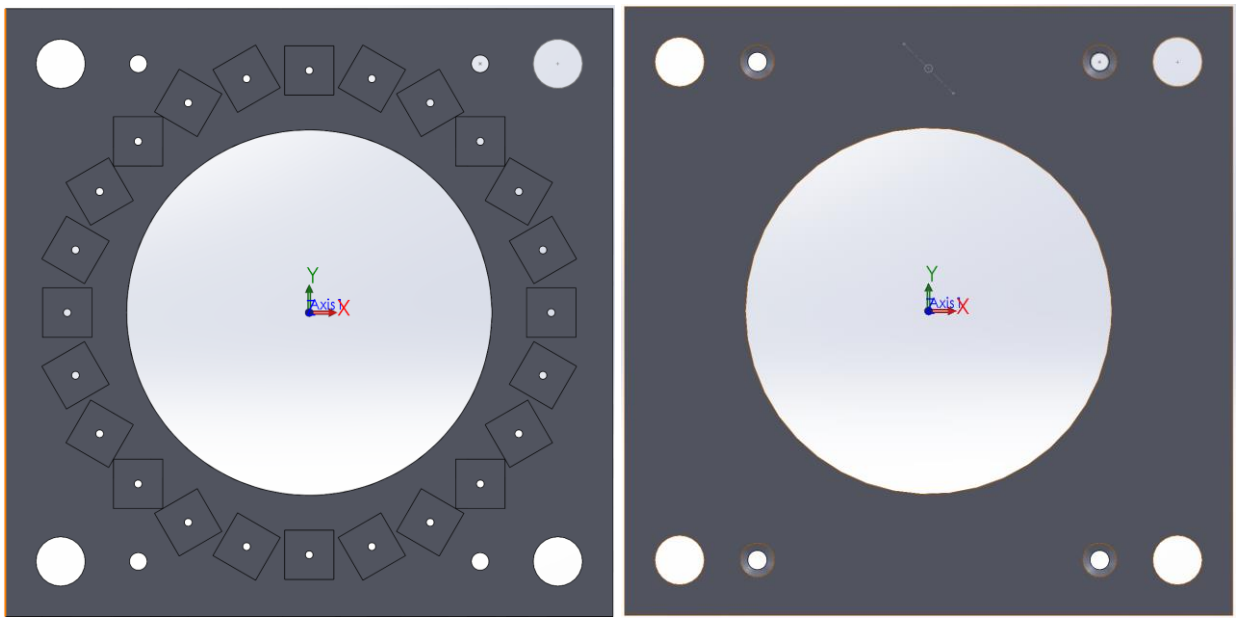

Fig. A3: n = 24 magnet former drawings.

The design is very similar to that of the n = 16 magnet former. The square holes are ¼ inch cubic holes. The length and width are 78.19 mm, very similar to the n = 16 magnet. The center hole is 47.08 mm in diameter. The cap piece is again 1/32 inch thick and the slots piece is 5/32 inch thick. The other features are identical to that of the n = 16 magnet.

REFERENCES

1. Lauterbur, P.C., *Image formation by induced local interactions: Examples employing nuclear magnetic resonance.* Nature, 1973. **242**(5394): p. 190-191.

2. Lauterbur, P.C., *Medical imaging by nuclear magnetic resonance zeugmatography.* Nuclear Science, IEEE Transactions on, 1979. **26**(2): p. 2807-2811.

3. Lauterbur, P.G. and C.-M. Lai, *Zeugmatography by reconstruction from projections.* Nuclear Science, IEEE Transactions on, 1980. **27**(3): p. 1227-1231.

4. Eidmann, G., et al., *The NMR MOUSE, a mobile universal surface explorer.* Journal of Magnetic Resonance, Series A, 1996. **122**(1): p. 104-109.

5. Blümich, B., et al., *The NMR-mouse: construction, excitation, and applications.* Magnetic resonance imaging, 1998. **16**(5): p. 479-484.

6. Blümich, B., et al., *Simple NMR-mouse with a bar magnet.* Concepts in Magnetic Resonance, 2002. **15**(4): p. 255-261.

7. Wright, S.M., et al., *A desktop magnetic resonance imaging system.* Magnetic Resonance Materials in Physics, Biology, and Medicine, 2001. **13**: p. 9.

8. Sahebjavaher, R.S., K. Walus, and B. Stoeber, *Permanent magnet desktop magnetic resonance imaging system with microfabricated multiturn gradient coils for microflow imaging in capillary tubes.* Review of Scientific Instruments, 2010. **81**(2): p. 023706.

9. Nacev, A., et al. *A quiet, fast, high-resolution desktop MRI capable of imaging solids*. in *Proceedings of the International Society for Magnetic Resonance in Medicine*. 2014.

10. Raich, H. and P. Blümler, *Design and construction of a dipolar Halbach array with a homogeneous field from identical bar magnets: NMR Mandhalas.* Concepts in Magnetic Resonance Part B: Magnetic Resonance Engineering, 2004. **23B**(1): p. 16-25.

11. Bluemler, P. and H. Soltner, *Dipolar Halbach Magnet Stacks Made from Identically Shaped Permanent Magnets for Magnetic Resonance.* Concepts in Magnetic Resonance Part A. **36A**(4): p. 12.

12. Danieli, E., et al., *Mobile sensor for high resolution NMR spectroscopy and imaging.* Journal of Magnetic Resonance, 2009. **198**(1): p. 80-87.

13. Kimura, T., et al., *Development of a mobile magnetic resonance imaging system for outdoor tree measurements.* Review of scientific instruments, 2011. **82**(5): p. 053704.

14. Windt, C.W., et al., *A portable Halbach magnet that can be opened and closed without force: The NMR-CUFF.* Journal of Magnetic Resonance, 2011. **208**: p. 27-33.

15. Cooley, C.Z., et al., *Two-dimensional imaging in a lightweight portable MRI scanner without gradient coils.* Magn Reson Med, 2015. **73**(2): p. 872-83.

16. Cooley, C.Z., *Portable low-cost magnetic resonance imaging*. 2014, Massachusetts Institute of Technology.

17. Sun, N., et al., *Palm NMR and 1-chip NMR.* Solid-State Circuits, IEEE Journal of, 2011. **46**(1): p. 342-352.

18. Lee, H., et al., *Chip–NMR biosensor for detection and molecular analysis of cells.* Nature medicine, 2008. **14**(8): p. 869-874.

19. Filippi, C., et al., *Proton MR Spectroscopy in a 1T Open MR Imaging System.* American Journal of Neuroradiology, 2011. **32**(8): p. E156-E159.

20. Halbach, K., *Design of permanent multipole magnets with oriented rare earth cobalt material.* Nuclear instruments and methods, 1980. **169**(1): p. 1-10.

21. Hills, B., K. Wright, and D. Gillies, *A low-field, low-cost Halbach magnet array for open-access NMR.* Journal of Magnetic Resonance, 2005. **175**(2): p. 336-339.

22. Zhang, X., et al. *Design, construction and NMR testing of a 1 tesla Halbach Permanent Magnet for Magnetic Resonance*. in *COMSOL Users Conference, Boston*. 2005.

23. Chang, W.-H., J.-H. Chen, and L.-P. Hwang, *Single-sided mobile NMR with a Halbach magnet.* Magnetic resonance imaging, 2006. **24**(8): p. 1095-1102.

24. Anderson, W.A., *Electrical current shims for correcting magnetic fields.* Review of Scientific Instruments, 1961. **32**(3): p. 241-250.